THE LANCET
Infectious Diseases

Supplementary appendix

This appendix formed part of the original submission and has been peer reviewed. We post it as supplied by the authors.

Supplement to: Kokaliaris C, Garba A, Matuska M, et al. Effect of preventive chemotherapy with praziquantel on schistosomiasis among school-aged children in sub-Saharan Africa: a spatiotemporal modelling study. *Lancet Infect Dis* 2021; published online Dec 2. https://doi.org/10.1016/S1473-3099(21)00090-6.

Appendix

Search strategy, selection criteria and data extraction protocol

We did a systematic review following the PRISMA guidelines [10]. We searched for relevant publications pertaining to prevalence of *Schistosoma* spp infection in sub-Saharan Africa, in PubMed, ISI Web of Science, and African Journals Online, from January 1, 2000 to May 29, 2020. The application that supports the data compilation carries automated routines that flag duplicated entries according to survey year and locations within a district for each newly acquired reference.

We applied the search string "schisto* (OR mansoni, OR bilhar*, OR haema*) AND sub-Saharan Africa (OR Angola, OR Benin, OR Botswana, OR Burkina Faso, OR Burundi, OR Cameroon, OR Central African Republic, OR Chad, OR Congo*, OR Cote d'Ivoire, OR Cote d'Ivoire, OR Ivory Coast, OR Djibouti, OR Eritrea, OR Ethiopia, OR Gabon, OR Gambia, OR Ghana, OR Guinea*, OR Kenya, OR Lesotho, OR Liberia, OR Madagascar, OR Malawi, OR Mali, OR Mauritania, OR Mozambique, OR Namibia, OR Niger, OR Nigeria, OR Rwanda, OR Senegal, OR Sierra Leone, OR Somalia, OR South Africa, OR Sudan, OR Swaziland, OR Tanzania, OR Togo, OR Tunisia, OR Uganda, OR Zambia, OR Zimbabwe)". Government reports and other grey literature (eg, PhD theses, working papers from research groups, or unpublished research reports obtained through personal communication) were also considered.

We set no parameters for language or study design. We initially screened titles and abstracts to identify potentially relevant articles. We excluded case reports, invitro studies, non-human studies, or those that did not report on schistosomiasis. We additionally excluded studies without prevalence data, those done in specific groups of patients (eg, hospital patients, those infected with HIV) or clearly defined population groups (ie. travelers, military personnel, expatriates, nomads, and displaced or migrating populations, pregnant women, neonates) not representative of the general population, studies that used either indirect diagnostic techniques (because such tests distinguish between active and cleared infection) or direct stool smear (because of low diagnostic sensitivity), reports of case-control studies, clinical trials, pharmacological studies (except control groups without anthelmintic intervention), intervention studies (except for baseline data or control groups), studies that reported on species other than *S haematobium* and *S mansoni*, and surveys done before 2000, that were not community based or school based, or were done in places where population deworming had been done within 1 year, or study findings reported aggregated within regions (ie, administrative division of level one).

Full-text reports for potentially relevant papers were obtained and screened. We reviewed the reference lists of full-text articles for further possible data sources. Duplicates were removed. If important information was missing (eg, survey year, location names or coordinates, numbers of individuals assessed and positive, etc) or if surveys were aggregated, we contacted the authors for clarification. The survey locations were geographically referenced if this information was not provided in the data source or validated. The georeferencing was done using online maps and travel guide sources (e.g. Google maps, Wikimapia, iGuide Interactive Travel Guide, Humanitarian Data Exchange). We assigned centroids for administrative units on the basis of administrative boundaries in the Database of Global Administrative Areas (version 2).

Relevant survey data were extracted and entered in the GNTD database with information on the source (authors, journal, publication date), survey (date, type of survey), location (coordinates, name, administrative unit), and parasitology (species, number of people positive or examined, prevalence, age, diagnostic tool).

Quality control for each country was done by rechecking 30% of randomly selected papers deemed irrelevant. If any misclassifications were identified, the selection for the whole country was rechecked.

We included those surveys in the meta-analysis with sample size greater than ten individuals. If the date of the survey was missing, we used date of publication instead.

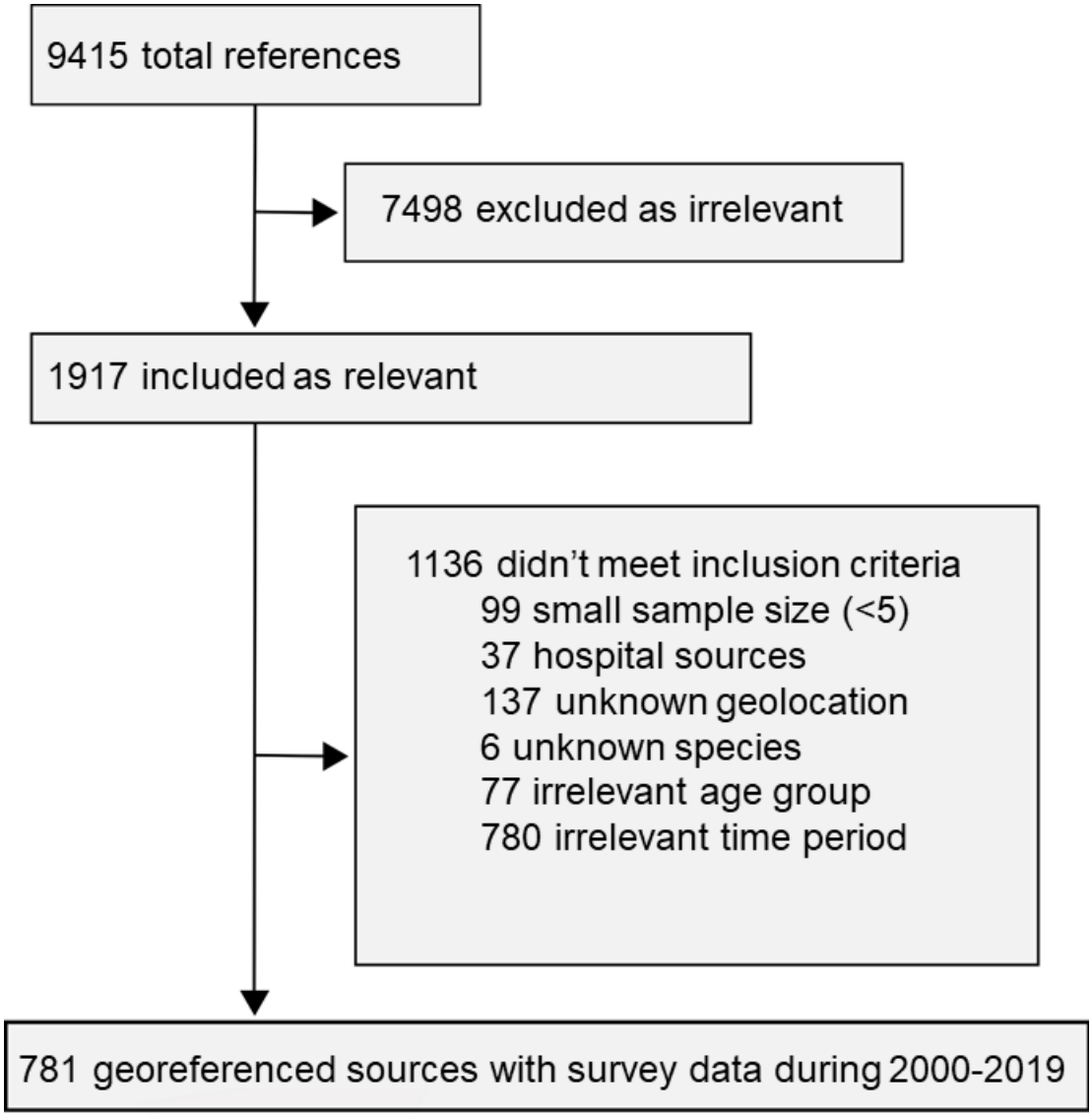

Figure A.1: Data search and selection criteria during 2000-201.

Data sources

Day and night land surface temperature (LSTD, LSTN) were used as proxies of ambient temperature. The normalized difference vegetation index (NDVI) was considered as a proxy for moisture. Decadal rainfall averages were obtained from the Climate Prediction Center rainfall estimates. In order to increase the predictive ability of the model, we also included 19 bioclimatic variables from the Worldclim database (http://www.worldclim.org/bioclim, accessed May 2020) into our analysis. Data on freshwater bodies were obtained from Copernicus Global Land Service (https://land.copernicus.eu/global/products/wb, accessed May 2020). The geographical distribution of socioeconomic and environmental predictors across SSA is displayed in Figure A.5 and A.6 respectively (pages 36, 47). Agro-ecological zones are presented in Figure A.7 (page 39) and were obtained from the International Food Policy Research Institute [32].

Data type	Data period	Temporal resolution	Spatial resolution	Source
Bioclimatic variables	1970-2000	Monthly	1 km	Worldclim - Global climate data version 2
Land surface temperature day and night	2000-2019	8 days	1 km	Moderate resolution imaging spectroradiometer (MODIS)/ Terra
Normalized difference vegetation index	2000-2019	16 days	1 km	MODIS/Terra
Land cover	2000-2019	Yearly	1 km	MODIS/Terra
Rainfall	-	Daily	15 km	Climate Prediction Center (CPC) Rainfall Estimator (RFE)
Altitude	-	-	90 m	Shuttle Radar Topography Mission (SRTM)
Rural - Urban	2000	-	1 km	Socioeconomic Data and Applications Center (SEDAC)
Population counts per pixel	2010-2020	-	100 m	WorldPop
Improved water source	2000-2017	-	Household surveys	Demographic and Health Surveys (DHS), Multiple Indicator Cluster Surveys - UNICEF, World Health *Surveys - WHO*
Improved sanitation	-	-		
Infant mortality rate	-	-		
Gridded surface of freshwater bodies	2019	-	300 m	Copernicus Global Land Service
Gridded surface of agro-ecological zones in Africa	2011	-	5 km	HarvestChoice/IFPRI 2009

Table A.1: Data sources and properties on socioeconomic and environmental explanatory variables.

	Locations						Positive diagnose (%)		
Country	Total	School	Community	2000-2010	2011-2014	2015-2019	2000-2010	2011-2014	2015-2019
Angola	431	41	390	41	182	206	76.6	17.9	7.5
Benin	384	1	383	6	184	194	43.4	20.9	15.4
Botswana	45	0	45	0	0	45			4.2
Burkina Faso	205	1	204	123	24	95	17.6	7.9	1.8
Burundi	22	0	22	22	0	0	0		
Cameroon	937	2	935	264	343	333	14.8	11.6	4.1
Central Africa	2	0	2	0	0	2			54
Chad	265	0	265	19	0	246	21.6		23.8
Ivory Coast	1192	15	1177	34	1133	26	24	4.5	3.6
Congo DR	2129	0	2129	9	304	1816	0	3.1	5.8
Equatorial Guinea	88	0	88	88	0	0	0.4		
Eritrea	40	0	40	40	0	0	0		
Ethiopia	10	1	9	2	8	0	25	21.9	
Gabon	220	0	220	2	218	0	47.4	5.8	
Gambia	209	0	209	0	0	209			5.1
Ghana	250	1	249	174	2	154	22.8	23.9	7.4
Guinea	117	10	107	37	8	80	22.6	0.7	14.1
Guinea-Bissau	117	0	117	0	1	116		20	2.6
Kenya	442	28	414	229	194	12	27.1	10.8	5.4
Liberia	604	0	604	0	503	101		1.4	27.8
Madagascar	178	2	176	2	0	176			33.2
Malawi	802	3	799	46	362	550	25.9	12.5	6
Mali	334	9	325	225	24	84	37.7	24.1	20.7
Mauritania	92	3	89	21	1	70	27.1	4	16.2
Mozambique	315	150	165	6	158	150	53.8	52.6	40.4
Namibia	380	0	380	0	296	84		5	9.5
Niger	1333	235	1098	462	709	265	30.2	13.1	10.4
Nigeria	2676	63	2613	235	2348	82	17.7	11.7	11.6
Rwanda	140	0	140	140	0	0	0		
Senegal	554	23	531	334	115	99	31.5	10.4	10.7
Sierra Leone	22	0	22	8	0	14	0		1.5
Somalia	28	4	24	0	25	0		10.4	
South Africa	309	0	309	3	1	306	33	26	2.1
South Sudan	224	0	224	76	0	148	4.3		0.7
Sudan	126	2	124	99	58	2	13	7.4	5
Swaziland	253	1	252	5	0	247	6.3		0.1
Tanzania	662	64	598	196	61	368	28.3	8.4	1.5
Togo	2185	0	2185	1090	1	1094	20.2	20.7	4.2
Uganda	75	11	64	72	0	0	0.6		
Zambia	672	7	665	103	555	14	23.9	12.4	17.4
Zimbabwe	416	10	406	287	1	0	24.3	25.3	
Total	19485	687	18798	4500	7819	7726	21.85	12.8	9.94

(a) S. haematobium

	Locations						Positive diagnose (%)		
Country	Total	School	Community	2000-2010	2011-2014	2015-2019	2000-2010	2011-2014	2015-2019
Angola	384	0	384	0	179	205		8.6	0.4
Benin	387	7	380	8	185	194	0	2.8	1
Botswana	125	0	125	1	0	124	0		0.5
Burkina Faso	202	0	202	102	21	95	3.6	1.3	0.2
Burundi	211	0	211	22	189	0	4.1	1.9	
Cameroon	918	3	915	251	342	327	10.6	6.2	2.4
Central Africa	30	0	30	0	0	30			52.6
Chad	247	1	246	1	0	246			1
Ivory Coast	1536	19	1517	115	1396	26	31.7	12.4	8.9
Congo DR	2147	0	2147	9	314	1824	57.6	3.8	6.6
Equatorial Guinea	88	0	88	88	0	0	0.2		
Eritrea	335	0	335	40	151	146	2.4	3.1	1
Ethiopia	2326	19	2307	174	2133	13	18.6	6.9	25.8
Gabon	22	0	22	0	22	0		0.1	
Gambia	209	0	209	0	0	209			0.1
Ghana	127	0	127	78	2	82	3.4	27.9	3.7
Guinea	117	10	107	37	8	80	66.2	2.4	28
Kenya	1812	159	1653	681	881	118	15.4	24.7	15.8
Liberia	1128	0	1128	0	1042	86		11.6	19.3
Madagascar	242	0	242	0	1	241		15.2	17.1
Malawi	754	3	751	30	328	537	0.5	5	1.3
Mali	324	6	318	216	24	84	7.2	4.5	3
Mauritania	66	4	62	11	0	55	4.7		0
Namibia	295	0	295	0	295	0		4.1	
Niger	150	14	136	136	0	13	1.3		
Nigeria	2347	21	2326	44	2227	75	9.6	1.4	4.1
Rwanda	326	0	326	142	183	1	3	2	8.3
Senegal	257	14	243	51	105	100	44.7	0.5	0.6
Sierra Leone	103	0	103	79	10	14	25	4.3	11.9
South Africa	298	0	298	1	0	297	16.6		0.2
South Sudan	425	0	425	206	0	219	9.2		3.7
Sudan	43	2	41	40	1	1	13.1	22.5	11.6
Swaziland	247	0	247	0	0	247			0.3
Tanzania	919	213	706	143	223	372	12.7	42.5	9.8
Togo	2190	0	2190	1090	1	1099	3.4	16.1	0.8
Uganda	1720	83	1637	606	292	803	20.7	26.4	12.5
Zambia	661	13	648	86	558	14	8.5	12	5.9
Zimbabwe	404	6	398	279	1	0	8.6	0	
Total	24122	597	23525	4767	11114	8315	13.5	13.02	6.11

(b) S. mansoni

Table A.2: Overview of survey data in SSA for *S. haematobium* (left) and *S. mansoni* (right) during 2000-2019. Prevalence estimated from the raw survey data i.e. total positives out of total screened by period and country.

Bayesian modelling

Stationary model

Let y_j be the number of *Schistosoma* positive cases out of the N_j examined individuals at location $j = 1,2, \dots n$ and survey period t, where t is an indicator variable for the time period with 2000-2010 as the baseline and dummy variables for 2011-2014 and 2015-2019. We assume that y_j follows a Binomial distribution with prevalence p_j and use the logit link function to relate the disease prevalence with its predictors, that is:

$$\begin{matrix} y_j & \sim Binomial(p_j, N_j), \\ logit(p_j) & \beta x_j + bt + \xi_j + e_j. \end{matrix} \quad 12$$

The vector x_j contains the values of the predictors at location j and time t. The regression coefficients β and b represent the effects of the predictors and the global time trend, respectively. Non-spatial variation is captured through the pure noise term e_j. In order to take into account potential spatial correlation, we included in the model a random spatial term ξ_j at unique location j and assumed that $\xi = (\xi_1, \xi_2, \dots \xi_n)$ is a zero mean, and stationary Gaussian random process $\xi \vee \sigma, \rho \sim N(0, \Sigma(\sigma, \rho))$ with a Matérn covariance function $C_\nu(d_{ij}) = \sigma^2 \frac{2^{1-\nu}}{\Gamma(\nu)}$, where Γ is the gamma function and $\Sigma(\sigma, \rho)$ is the covariance matrix with elements $c_{ij} = C_\nu(d_{ij})$, and d_{ij} is the Euclidian distance between two locations i and j, $K_\nu(x)$ the modified Bessel function of order ν, where ν determines the smoothness of the process. As ν increases, the function becomes more smooth, i.e $\nu = 0.5$ represents the exponential covariance function, and for $\nu \to \infty$ it approximates the Gaussian covariance function. The hyperparameters σ and ρ define the spatial variance and range (i.e. distance where spatial correlation is considered non-essential), accordingly. In our analysis we fixed $\nu = 1$ which leads to stable computations with INLA [33], while the spatial parameters σ and ρ are estimated in the process.

We assumed non-informative Gaussian prior distributions for the regression coefficients β and the global time trend b. Non-informative gamma prior distributions were considered for the hyper-parameters σ, ρ of the spatial process and σ_e of the pure noise (transformed on the logarithmic scale), that is $log\left(\frac{1}{\sigma^2}\right) \sim Ga(5 \times 10^{-5}, 1)$, $log(\rho) \sim Ga(0.01,1)$, and $log\left(\frac{1}{\sigma_e^2}\right) \sim Ga(5 \times 10^{-5}, 1)$.

Restricted spatial model

In order to account for spatial confounding due to multicollinearity between the spatial covariates $X = (x_j)$ and the spatial stochastic process ξ, we update the model in 2 by replacing the spatial process ξ with $\xi = (I - P_x)\xi$, where $P_x = X$ is the projection matrix and $(I - P_x)\xi$ is the orthogonal projection of the spatial process ξ on X.

Non-stationary model

Let $\xi = (\xi_1, \xi_2, \dots \xi_n)$ be a non-stationary Gaussian stochastic process, τ_j the local precision where j is a given location in space, and κ the spatial scale parameter associated empirically with the spatial range $\rho \approx \frac{\sqrt{8}}{\kappa}$, such that for $\nu = 1$ the spatial correlation is 0.1 at ρ distance [33]. Then we specify $log(\kappa) = \theta_1, log(\tau_j) = \theta z_j$, where vector z_j represents the values of the covariates for the spatial variance at location j. Now the spatial variance becomes $\sigma = (\sigma_1^2, \sigma_2^2, \dots \sigma_n^2)$, where $\sigma_j^2 \approx \frac{1}{4\pi\kappa^2\tau_j^2}, j = 1, \dots, n$ [33]. We conclude the Bayesian specification by

assuming non-informative Gaussian prior distributions for the hyper parameters θ_1 and θ.

Spatio-temporal model

Let $\phi = (\phi_{jt}), j = 1,2,\dots,n, t = 1,2,\dots,T$ be a stochastic process accounting for correlation in space and time, for n unique locations and T time-points [18]. The spatio-temporal process ϕ_{jt} changes in time through a first order autoregressive process (AR1):

$$\phi_{jt} = \begin{cases} \xi_{j1}, & t = 1 \\ a\phi_{j,t-1} + \xi_{jt}, & t = 2,\dots,T \end{cases}$$

where a is the temporal lag with $a \vee 1$ and ξ a pure spatially structured term with $\xi = (\xi_{jt}), j = 1,2,\dots,n, t = 1,2,\dots,T$ which follows a zero-mean multivariate normal distribution as described in (1) with Matérn covariance function for $j_1 = j_2$:

$$Cov(\xi_{j_1,t_1}, \xi_{j_2,t_2}) = \begin{cases} \sigma^2 C_\nu(d_{j_1,j_2}), & t_1 = t_2 \\ 0, & t_1 = t_2 \end{cases}$$

Model selection and validation

Due to the large number of potential predictors, each of them was examined for multicollinearity with the remaining, excluding those with variance inflation factor >4. Bayesian geostatistical models were fitted with one predictor at a time, to identify the predictors functional form to be included in the final geostatistical predictive model. A linear and categorical form was considered for each predictor (categories corresponding to the quantiles of the predictor) and the form with lowest log CPO score was chosen [20, 23]. We identified a subset of 13 potential socioeconomic and environmental predictors (Appendix, Table A.4, page 31), which gave rise to a sample space of 8,192 possible models for *S. haematobium* and *S. mansoni*, respectively. We fitted all possible models for both *Schistosoma* infections. The models with highest predictive ability, were used for inference and predictions. Model validation was carried out by assessing the model's predictive performance. The models were fitted on a training set, including 90% of our survey locations, and their predictions were validated on a test set of the remaining locations. The mean absolute error (MAE), which is the average of the absolute differences between observed and predicted values, the % of prevalence correctly estimated within a 95% BCI and the % of prevalence underestimation were used to assess the out-of-sample performance of the models. Smaller values of MAE indicate smaller prediction error, the model predicts exactly the true value if MAE is equal to zero [34].

S. haematobiu MAE	Within BCI %	Underestimation %	*S. mansnoni* MAE	Within BCI %	Underestimation %
0.076	79.6	2.0	0.050	86.0	1.9
0.080	76.5	2.9	0.053	87.1	1.3
0.074	78.0	2.4	0.053	85.2	2.2
0.080	79.9	1.8	0.056	85.3	2.4
0.084	79.0	2.4	0.052	86.3	2.1
0.082	78.7	2.8	0.053	85.3	1.9
0.079	75.6	2.6	0.053	86.0	1.7
0.078	77.9	2.1	0.044	85.6	1.7
0.084	76.4	2.8	0.056	87.0	2.0
0.078	76.9	2.3	0.053	83.6	2.3
0.084	75.6	2.5	0.047	85.7	1.7
0.078	78.5	1.9	0.051	85.4	1.7
0.084	77.5	2.3	0.052	84.9	2.1
0.076	78.9	2.1	0.050	85.1	2.2
0.076	76.1	1.9	0.053	85.4	1.9
0.082	78.0	2.2	0.050	86.5	1.7
0.080	76.3	1.5	0.050	85.9	1.6
0.081	75.6	2.9	0.056	82.7	2.3
0.080	78.8	2.8	0.051	85.6	2.1
0.081	75.6	2.8	0.048	86.3	1.5
0.080	77.5	2.4	0.052	85.5	1.9

Table A.3: Mean absolute error, percentage of prevalence inside 95% BCI and percentage of prevalence underestimation for *S. haematobium* and *S. mansoni*, from 20 repeated model validations leaving out 10% of data.

Number of infected school-aged children and estimated treatment needs

The models in (1) with the best set of explanatory variables obtained from the model selection were used to predict *S. haematobium* and *S. mansoni* prevalence across SSA on a 5 x 5 km grid of roughly 10 million pixels. A sample of 200 from the posterior predictive distribution was utilised to estimate population-adjusted prevalence and treatment needs at country level, together with their uncertainty. The predicted prevalence surfaces were overlaid with a population grid obtained from WorldPop (http://www.worldpop.org.uk/, accessed May 2020) providing population estimates at 100 x 100 m in 2010 and converted to number of infected people at pixel level in the WorldPop spatial resolution. Estimates of the number of infected people were aggregated at country level and divided by the total country population to obtain population-adjusted prevalence estimates. We obtained population estimates for the year 2019, by applying population growth rates obtained from the United Nations population prospects (https://population.un.org/wpp/, accessed 2020) to the 2010 data and assuming a linear population growth. The number of treatment needs for school-aged children (5-14 years) was calculated by categorising pixels into low (prevalence <10%), moderate (prevalence 10-50%) and high risk (prevalence >50%) categories and aggregating treatments at country level according to the number of infected individuals in each risk category, following WHO treatment guidelines [21].

Analyses were carried out using integrated nested Laplace approximations (INLA) [35] and the stochastic partial differential equations method (SPDE), [33] which were implemented in R software version 3.3.3 and the INLA package. The number of infected children was calculated at 100x100 m spatial resolution available for the population data, to reduce misclassification of population counts at the borders. These calculations were performed in Google Earth Engine. [36]

Variables	*S. haematobium*	*S. mansoni*
Annual mean temperature	-	-
Annual precipitation		Selected
Elevation	Selected	Selected
Infant mortality rate (IMR)	Selected	Selected
Isothermality		Selected
Land cover		
LST at day	Selected	-
LST at night	Selected	Selected
Max temperature of warmest month	-	-
Mean diurnal temperature range	Selected	
Mean temperature of coldest quarter	-	-
Mean temperature of driest quarter	Selected	Selected
Mean temperature of warmest quarter	-	-
Mean temperature of wettest quarter		Selected
Min temperature of coldest month	-	-
NDVI	Selected	Selected
Precipitation of coldest quarter	-	-
Precipitation of driest month	-	-
Precipitation of driest quarter	-	-
Precipitation of warmest quarter	-	-
Precipitation of wettest month	Selected	-
Precipitation of wettest quarter	-	-
Precipitation seasonality	-	-
Proportion of improved drinking water sources	Selected	Selected
Proportion of improved sanitation	Selected	Selected
Proportion of open defecation	Selected	Selected
Temperature annual range	-	-
Temperature seasonality	-	-
Agro-ecological zone	Selected	Selected
Urban extents	Selected	Selected

Table A.4: Predictors identified as important by variable selection and included in the final geostatistical models of *S. haematobium* and *S. mansoni*.

Country	2006	2007	2008	2009	2010	2011	2012	2013	2014	2015	2016	2017	2018
Angola	0.0	0.0	0.0	0.0	0.0	0.0	0.0	0.0	14.4	9.1	32.8	25.9	29.4
Benin	0.0	0.0	0.7	0.0	16.1	0.0	0.1	5.1	47.2	45.7	35.0	45	46.5
Botswana	0.0	0.0	0.0	0.0	0.0	0.0	0.0	0.0	0.0	0.0	0.0	0.0	0.0
Burkina Faso	24.5	6.4	28.4	23.2	100.0	82.4	79.6	96.4	62.4	94.5	70.6	92.6	100.0
Burundi	0.0	0.0	0.0	0.0	63.4	43.6	43.6	0.0	46.0	24.8	30.9	62.6	94.7
Cameroon	1.1	3.8	0.0	5.3	11.1	17.2	21.7	10	56.8	56.8	43.7	63.3	19.4
Central African Republic	0.0	0.0	0.0	4.5	26.4	0.0	30.1	7.8	9.4	0.0	39.4	0.0	15.9
Chad	0.0	0.0	0.0	0.0	0.0	0.0	0.0	0.0	0.0	0.0	0.0	57.7	45.3
Congo	0.0	0.0	0.0	0.0	0.0	0.0	0.0	0.0	2.0	54.9	18.2	40.8	37.4
Congo DR	0.0	0.0	0.0	0.0	0.0	0.0	0.0	0.0	11.9	12	42.1	57.8	49.2
Cote d'Ivoire	0.0	0.0	0.0	0.1	0.0	0.0	16.9	21.5	36.1	10.8	48.3	62.9	62.7
Equatorial Guinea	0.0	0.0	0.0	0.0	0.0	0.0	0.0	0.0	0.0	0.0	0.0	0.0	0.0
Eritrea	0.0	0.0	0.0	0.0	0.0	0.0	0.0	0.0	17.7	15.3	59.7	61.2	67.9
Eswatini	0.0	13.2	11.4	6.4	0.0	0.0	0.0	0.0	0.0	0.0	51.6	0.0	0.0
Ethiopia	0.0	0.0	0.0	0.0	0.0	0.0	0.0	4.5	7.6	28.8	29.2	47.3	48.0
Gabon	0.0	0.0	0.0	0.0	0.0	0.0	0.0	0.0	0.0	0.0	36.7	0.0	90.7
Gambia	0.0	0.0	0.0	0.0	0.0	0.0	0.0	0.0	0.0	0.0	0.0	83.3	0.0
Ghana	0.0	0.0	2.6	1.3	27.4	21.4	29.8	0.0	19.7	26.5	37.9	21.4	0.0
Guinea	0.0	0.0	0.0	0.0	0.0	0.0	33.5	0.0	0.0	0.0	31.2	42.7	47.1
Guinea-Bissau	0.0	0.0	0.0	0.0	0.0	0.0	0.0	0.0	0.0	38.5	0.0	0.0	97.9
Kenya	0.0	0.0	0.0	0.0	0.0	0.0	0.0	15.5	23.5	20.7	24.4	23.6	0.0
Liberia	0.0	0.0	0.0	0.0	0.0	0.0	30.9	29.0	0.0	0.0	12.8	15.5	79.2
Madagascar	0.0	0.0	6.8	5.3	13.7	6.7	2.9	15.4	26.5	17.9	19.1	46.9	0.0
Malawi	0.0	0.0	0.1	6.1	26.4	31.5	43.1	0.0	56.9	80.1	64.5	44.5	79.2
Mali	11.1	4.8	25.1	15.0	73.5	42.9	42.0	70.4	9.2	65.7	58.8	56.0	54.9
Mauritania	0.0	0.6	0.0	0.0	27.2	0.0	22.9	9.6	0.0	21.2	0.0	32.0	31.1
Mozambique	0.0	2.9	0.0	0.0	3.8	13.6	9.8	28.1	42.9	0.0	43.3	18.4	22.7
Namibia	0.0	0.0	0.0	0.0	0.0	0.0	0.0	0.0	0.0	0.0	0.0	0.0	0.0
Niger	15.3	12.3	11.4	12.4	51.1	23.1	78.5	42.4	92.4	54.7	0.0	97.7	100.0
Nigeria	0.1	0.1	0.8	0.8	4.0	2.7	5.4	5.9	11.0	31.3	39.9	55.3	45.3
Rwanda	0.0	0.0	20.1	27.6	0.0	0.0	15.8	24.7	7.6	12.7	0.0	40.3	50.4
Sao Tome and Principe	0.0	0.0	0.0	0.0	0.0	0.0	0.0	0.0	0.0	72.0	60.6	0.0	59.8
Senegal	0.1	0.0	0.0	3.3	14.2	0.0	29.0	42.3	51.2	55.7	19.3	49.5	32.1
Sierra Leone	0.0	0.0	0.0	11.2	99	100.0	98.9	93.2	0.0	100	81.8	99.8	0.0
Somalia	0.0	0.1	0.3	0.3	1.7	2	0.0	0.0	0.0	0.0	0.0	35.6	99.2
South Africa	0.0	0.0	0.0	0.0	0.0	0.0	0.0	0.0	0.0	0.0	0.0	0.0	0.0
South Sudan	0.0	0.0	0.0	0.0	0.0	0.0	0.0	0.0	16.1	0.0	0.0	0.0	0.0
Sudan	6.0	4.4	2.0	3.0	0.1	30.8	1.1	24.8	4.1	38.1	37.9	32.4	72.5
Tanzania	0.0	7.8	0.0	0.6	16.0	13.8	30.9	27.6	27.3	36.3	42.2	43.3	40.2
Togo	0.0	0.0	0.0	0.0	44.8	78.2	93.4	94.8	54	76.1	38.7	60.2	100
Uganda	1.9	0.0	5.9	12.7	32.9	17.6	18.6	0.0	26	36.2	36.7	51.9	55.5
Zambia	3.6	0.0	0.0	0.0	3.0	0.0	0.0	0.0	0.0	19.8	20.2	29.8	13.8
Zimbabwe	0.0	0.0	0.0	0.0	0.0	0.0	33.0	48.9	48.9	63.6	51.5	64.5	0.0

Table A.5: Schistosomiasis PC national treatment coverage for each sub-Saharan African country.

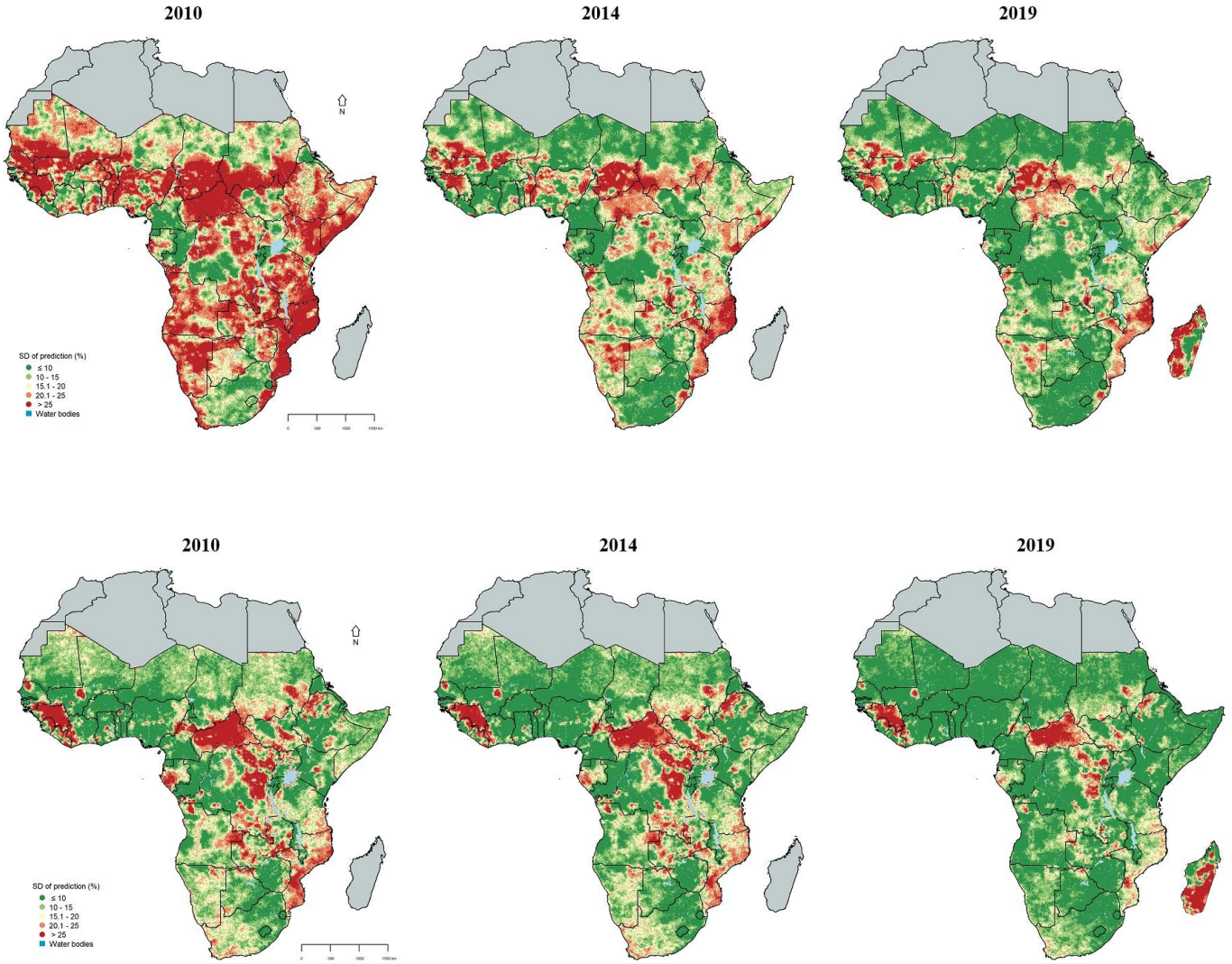

Figure A.2: Estimates of predictive uncertainty (posterior predictive standard deviation (SD)) for *S. haematobium* (top) and *S. mansoni* (bottom) across sub-Saharan Africa. Higher values of SD indicate larger prediction uncertainty for the prevalence at a given pixel. Practically, the prevalence at a given pixel varies between the predicted value plus or minus two units of SD.

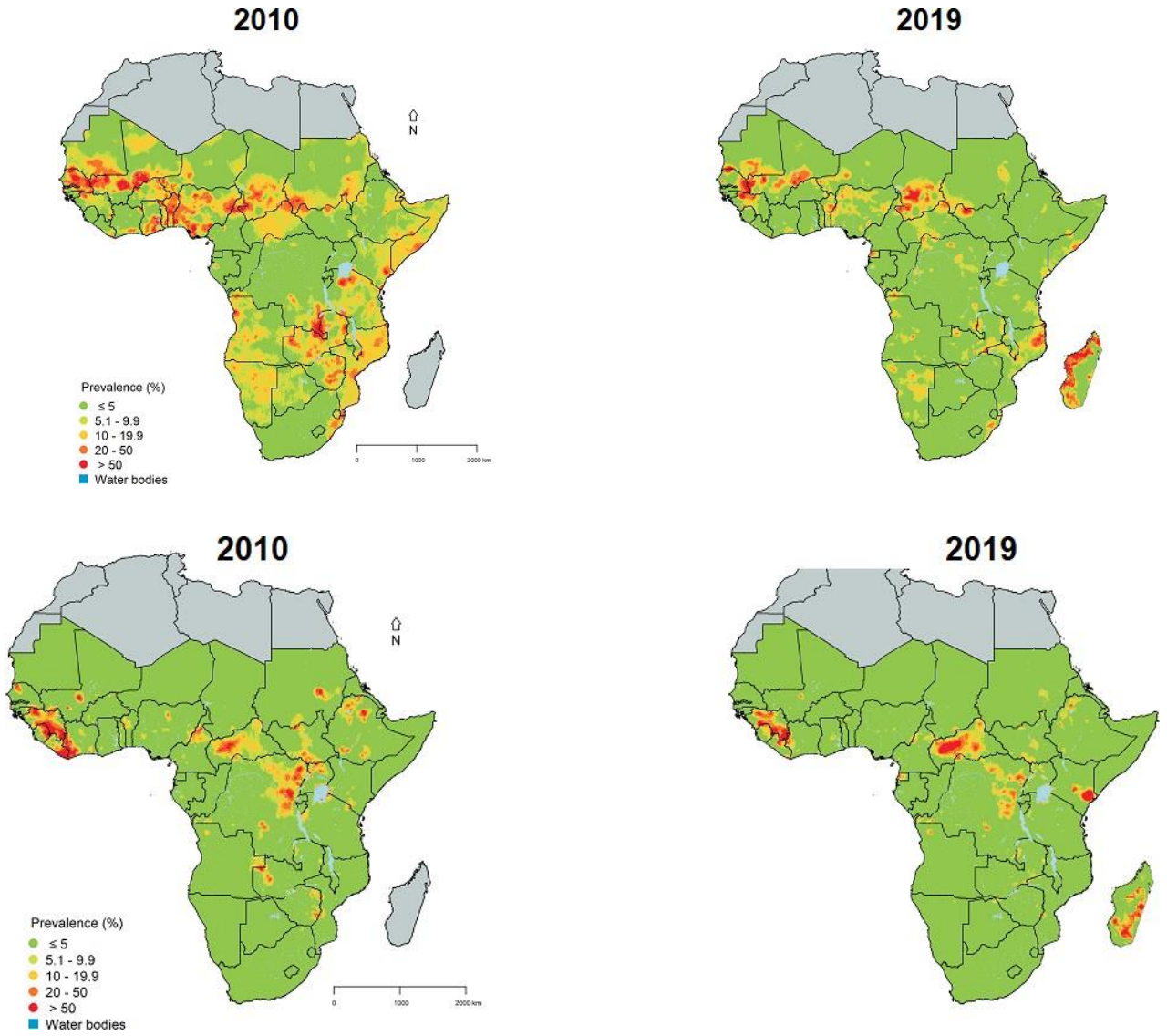

Figure A.3: Spatio-temporal model prevalence estimates (posterior predictive median) for *S. haematobium* (top) and *S. mansoni* (bottom) across sub-Saharan Africa.

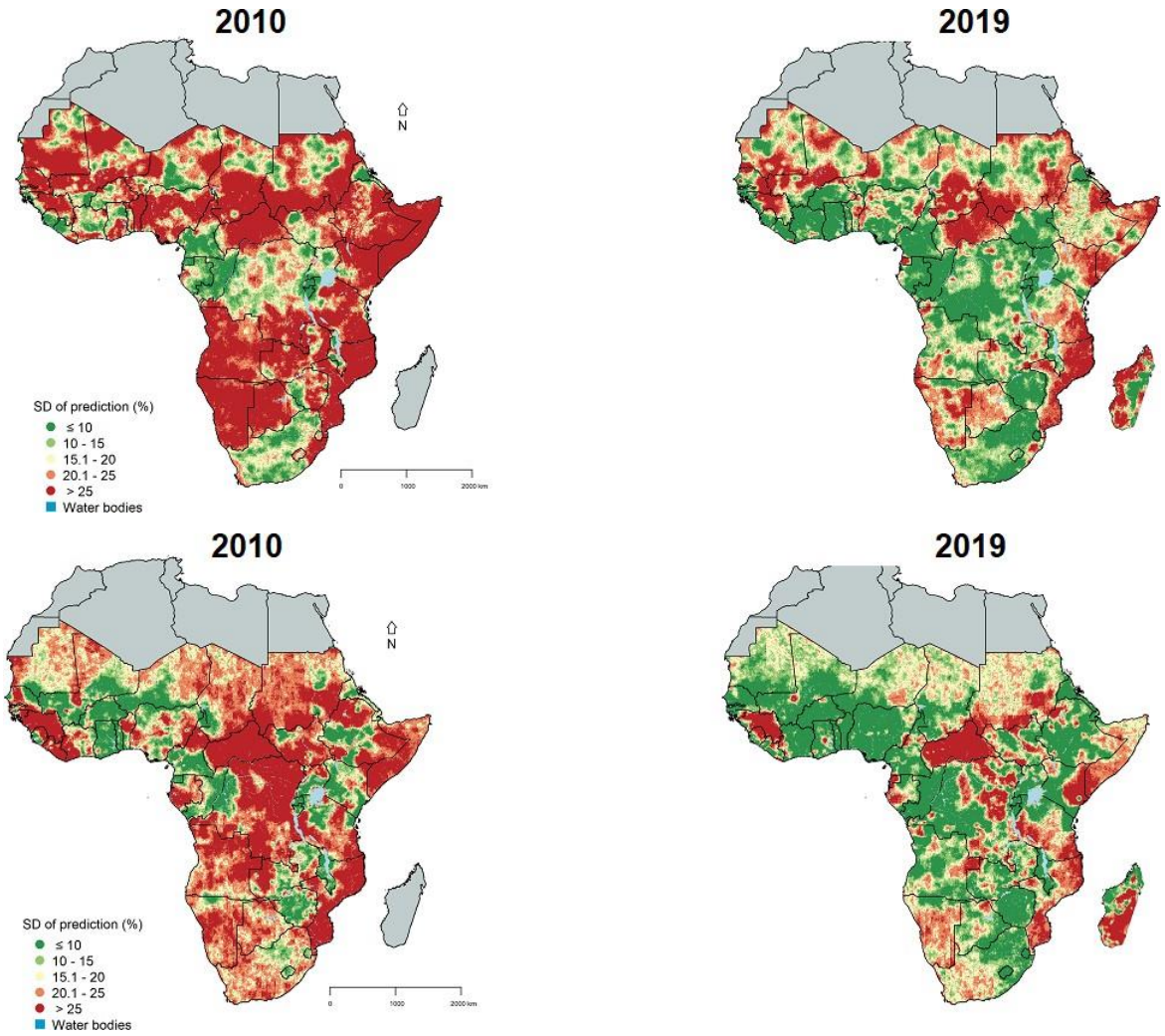

Figure A.4: Spatio-temproal model estimates of predictive uncertainty (posterior predictive standard deviation (SD)) for *S. haematobium* (top) and *S. mansoni* (bottom) across sub-Saharan Africa. Higher values of SD indicate larger prediction uncertainty for the prevalence at a given pixel. Practically, the prevalence at a given pixel varies between the predicted value plus or minus two units of SD.

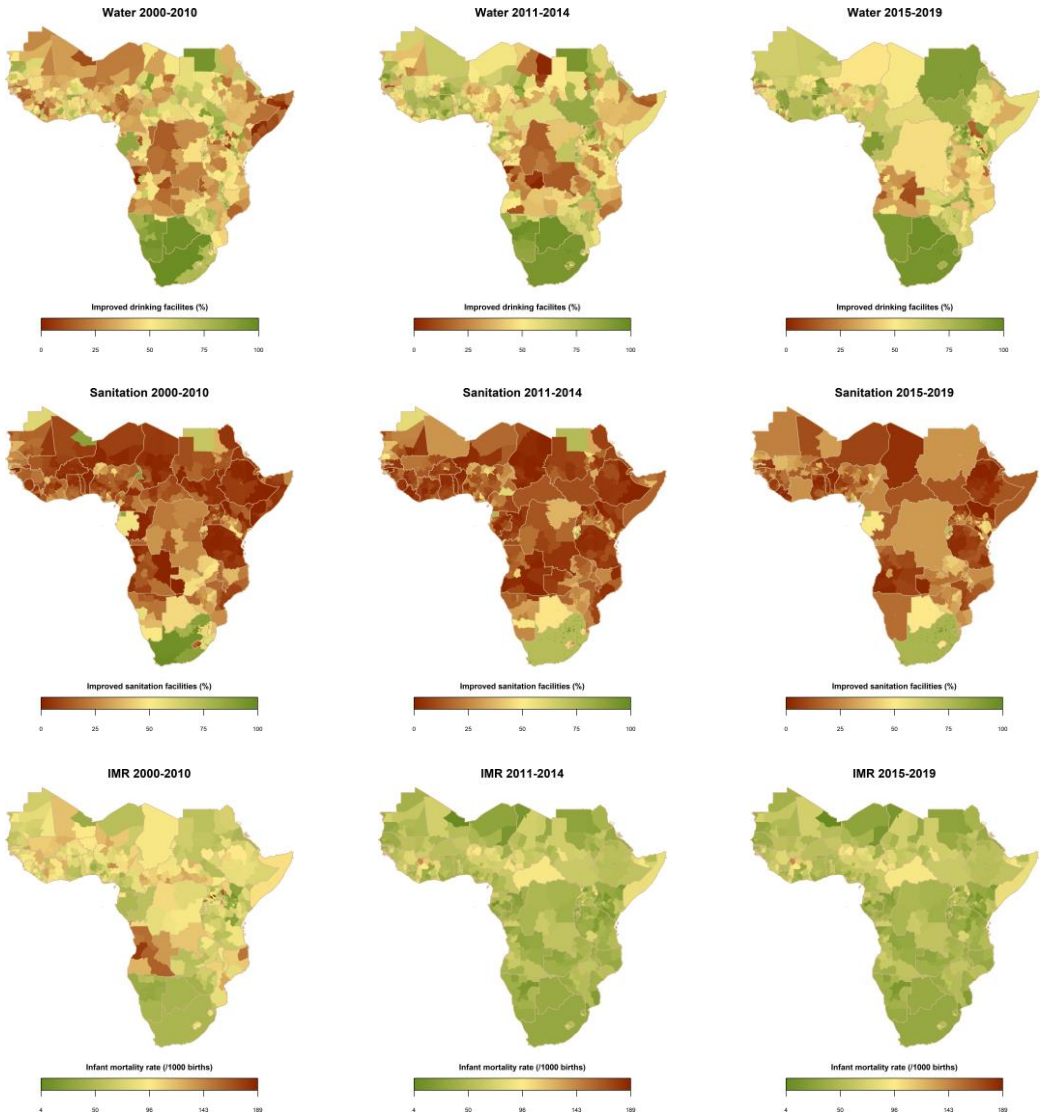

Figure A.5: Socioeconomic summaries across sub-Saharan Africa.

LST day 2000-2010

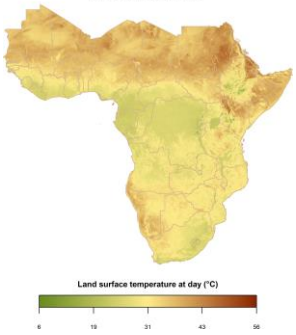

LST day 2011-2014

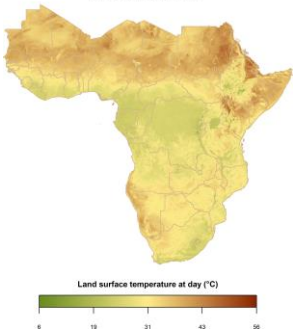

LST day 2015-2019

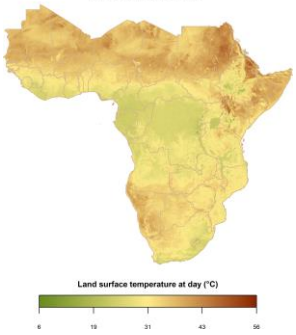

LST night 2000-2010

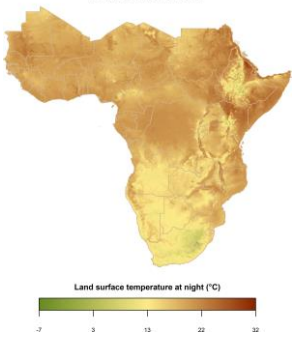

LST night 2011-2014

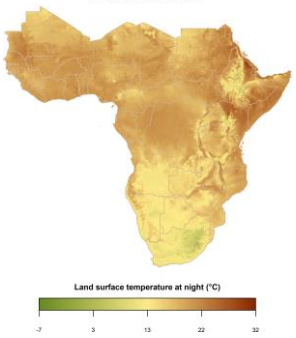

LST night 2015-2019

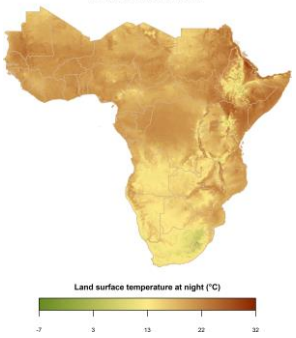

NDVI 2000-2010

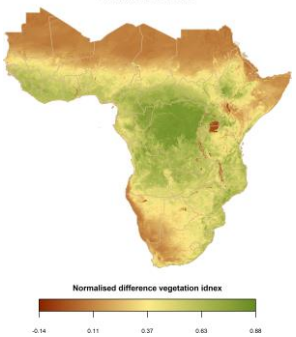

NDVI 2011-2014

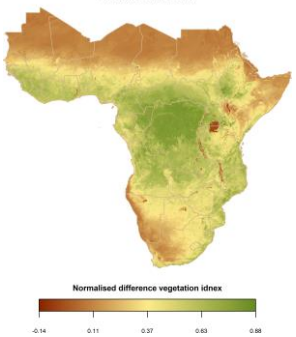

NDVI 2015-2019

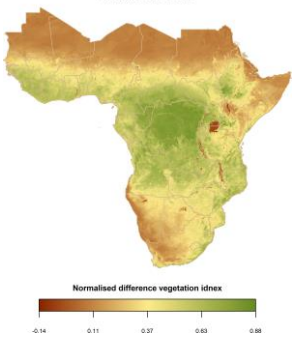

Rainfall 2000-2010

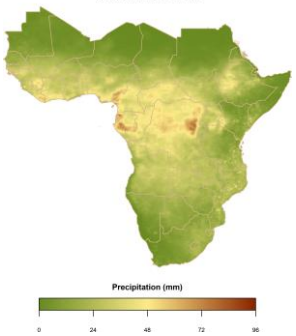

Rainfall 2011-2014

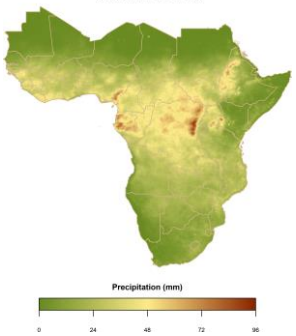

Rainfall 2015-2019

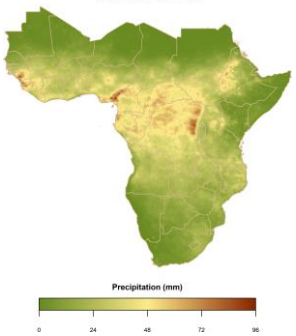

Altitude 2000-2010

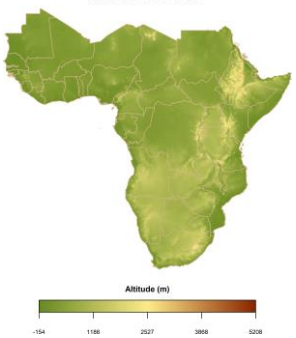

Altitude 2011-2014

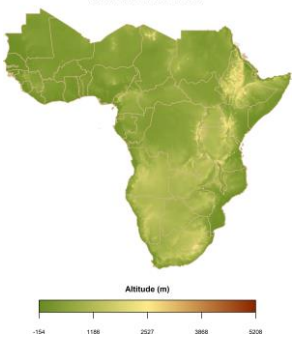

Altitude 2015-2019

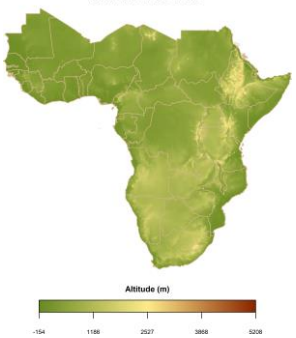

Figure A.6: Geographical distribution of environmental covariates across sub-Sahran Africa.

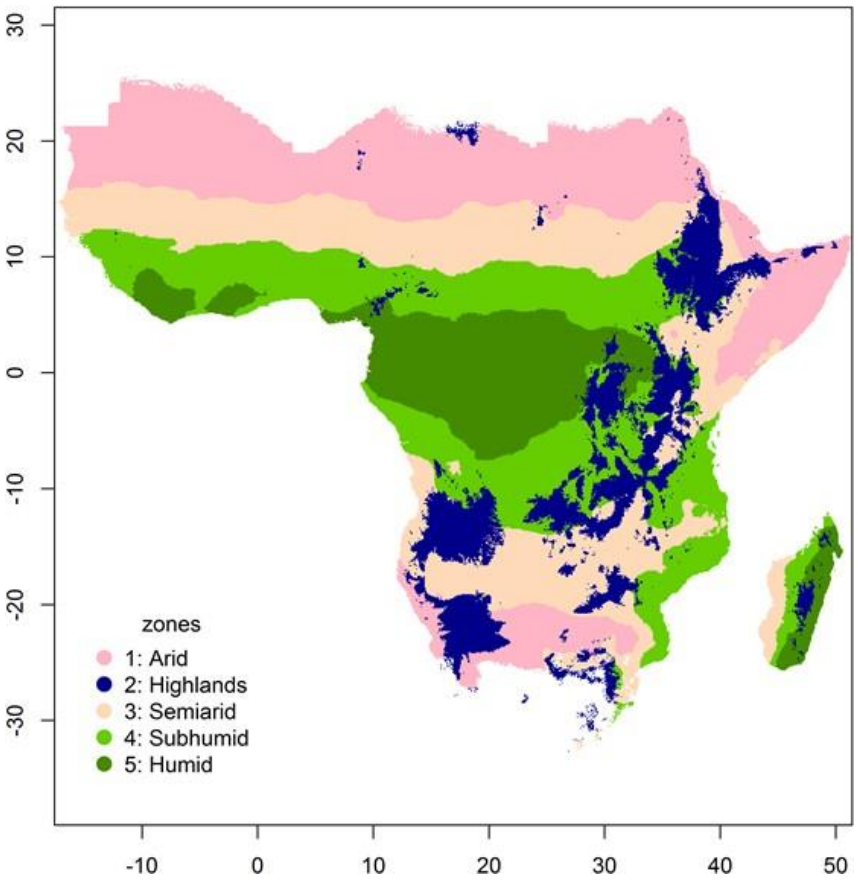

Figure A.7: Agro-ecological zones in sub-Saharan Africa.